THE JOURNAL OF PHYSICAL CHEMISTRY B

Article

pubs.acs.org/JPCB

Quantifying Coulombic and Solvent Polarization-Mediated Forces Between DNA Helices

Zhaojian He and Shi-Jie Chen*

Department of Physics and Department of Biochemistry, University of Missouri, Columbia, Missouri 65211, United States

Supporting Information

ABSTRACT: One of the fundamental problems in nucleic acids biophysics is to predict the different forces that stabilize nucleic acid tertiary folds. Here we provide a quantitative estimation and analysis for the forces between DNA helices in an ionic solution. Using the generalized Born model and the improved atomistic tightly binding ions model, we evaluate ion correlation and solvent polarization effects in interhelix interactions. The results suggest that hydration, Coulomb correlation and ion entropy act together to cause the repulsion and attraction between nucleic acid helices in Mg^{2+} and Mn^{2+} solutions, respectively. The theoretical predictions are consistent with experimental findings. Detailed analysis further suggests that solvent polarization and ion correlation both are crucial for the interhelix interactions. The theory presented here may provide a useful framework for systematic and quantitative predictions of the forces in nucleic acids folding.

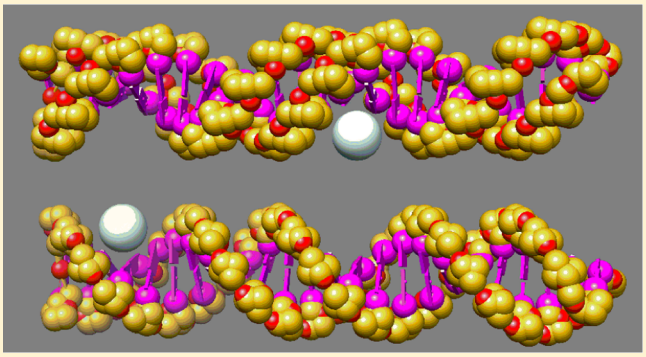

1. INTRODUCTION

Nucleic acids are charged polymers. Nucleic acid folding requires cations to neutralize the backbone charges. The cations in the solution can effectively screen Coulomb repulsion between the nucleotides.[1,2] Ion-mediated interactions between nucleic acids play crucial roles in cellular activities such as DNA condensation, packaging[1,2] and RNA folding.[3,4] Understanding the physical mechanism for ion-mediated nucleic acid interactions can have far-reaching impact on our ability to predict and analyze nucleic acid-related cellular functions. One of the intriguing ion effects is the ion-induced attraction between like-charged nucleic acid helices and triplexes.[5−14,16−30] Previous studies showed that the attractive force cannot be explained by Poisson−Boltzmann (PB)-like mean-field interactions between the charges, where fluctuations of ion distribution and correlations between the ions are ignored.[31,32] The result suggests that other effects, such as the fluctuations of charge density with the distance from the nucleic acid surface[6] and the two-dimensional (2D) ordering of ions on the nucleic acid surface,[7] may be responsible for the attractive force. Further investigations suggest that discrete DNA charges can lead to specific ion binding properties such as binding to the grooves (vs binding to phosphate charges) and the resultant charge modulation may cause attraction between nucleic acids.[8−13]

A series of excellent biophysical experiments such as osmotic stress measurements suggest that hydration effect may be responsible for the nucleic acids attractions.[14,16,17] However, due to the complex interplay between the different forces such as the Coulombic force, the hydration force, and the ionic entropic force, a detailed quantitative analysis of the mechanism remains a challenge.[1,5,16−25] One of the key issues is how to quantify the different forces. The objective of this paper is to provide a quantitative analysis for the physical mechanism of the forces responsible for the possible interhelix attraction.

Previous theoretical studies have suggested that correlations and fluctuations of multivalent ions around the nucleic acids could induce an attractive force between the nucleic acids.[8−11] However, the previous theories were mostly based on various simplified structural models for nucleic acids. Recently, a new theory, called "the tightly bound ion" (TBI) theory,[33] was developed to account for ion correlations and fluctuations. Compared with the previous simplified models for ion correlation, the TBI theory has the advantage to treat realistic 3D structures of the nucleic acids. The TBI theory predicted that DNA double helices can attract each other in divalent ion solutions such as Mg^{2+} solutions.[10] The conclusion is not fully consistent with the experimental finding, which showed a repulsive interaction between helices in a Mg^{2+} solution.[14] This theory-experiment difference may provide insights into the mechanism for the interplay between the different forces between the helices.

Two possible problems with the previous TBI predictions are (a) the use of a coarse-grained structural model for the nucleic acids and (b) lack of the hydration effect. To find out the dominant reason that causes the inconsistency between the

Received: January 31, 2013
Revised: May 21, 2013
Published: May 24, 2013

 © 2013 American Chemical Society dx.doi.org/10.1021/jp4010955 | J. Phys. Chem. B 2013, 117, 7221−7227

previous theoretical predictions and the experimental results, we performed calculations using the all-atom (instead of coarse-grained) structure-based TBI model.[15,34] The all atom-based theory again predicts an attractive force in a Mg^{2+} solution (see below), which shows that lack of hydration effect (instead of the use of coarse grained structure) may be the dominant reason. The above test result points to the possible indispensable role of the hydration effect, along with other effects such as the ion correlation effect, in the interactions between nucleic acids. The conclusion about the importance of the hydration effect is consistent with the findings from the previous biophysical experiments.[16,17,20] In this paper, through an atomistic structure-based analysis for the solvent hydration and the ion correlation effects, we quantify the different components of the ion-mediated forces between DNA helices and investigate how the integration of the above effects leads to the experimentally observed forces between DNA helices.

2. METHODS AND RESULTS

Prediction of the Electrostatic Free Energy through Integration of the Tightly Bound Ion (TBI) Model and the Generalized Born (GB) Model. We consider a pair of 24-base pair double-stranded DNA helices (dsDNAs) immersed in an ionic solution (Figure 1a); See the Supporting Information (SI) "Helix24.pdb" for the PDB coordinates of the structure. The all-atom dsDNAs are generated by the software X3DNA.[35] To evaluate the interaction between the helices, we compute the free energy of the system as a function of helix–helix distance x. We use the recently developed atomistic improved TBI model[34] to treat the electrostatic correlation effect in multivalent ionic solution; see the SI for a description of the TBI model. Briefly, in the TBI model, we separate out a region, called the "tightly bound" (TB) region, from the rest region (called the "diffusive" region) in the solution. The TB and the diffusive regions are defined as regions where Coulomb correlation between ions is strong and weak, respectively. The TB region, depending on the ionic condition of the solution, is usually a thin layer around the nucleic acid structure. For ions in the TB region ("TB ions"), we enumerate all of the discrete modes for the many-ion distributions and account for ion correlation through many-ion Coulomb energy for each mode. For ions in the diffusive region, we apply the Poisson–Boltzmann (PB) theory.[10] The statistical average over all of the ion binding modes determines the thermodynamic stability of the system.

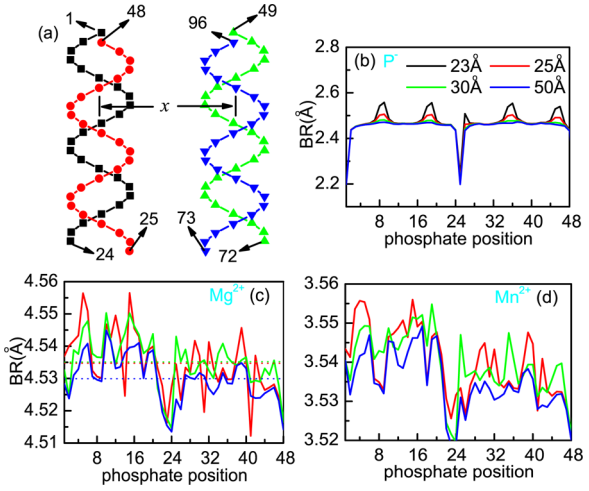

Figure 1. (a) System of two 24-bp dsDNA helices. The numbers mark the sequence of the phosphates. The Born radii of the phosphates (b), Mg^{2+} (c), and Mn^{2+} (d) for the different interaxial separations. The same color indicates the same interaxial distance x.

We consider both the nonpolar and polar contributions to the hydration effect. As a crude approximation, we use the generalized Born (GB) model[36−38] and the solvent accessible surface area-based model[39−42] to estimate the polar and the nonpolar free energies, respectively. We first include the polar contribution in the atomistic TBI model. We will then evaluate the importance of the nonpolar effect through quantitative estimations, which suggest that the inclusion of the nonpolar contribution does not alter the conclusions.

The electrostatic energy for the charges (phosphates, TB ions) in the TB region for a given binding mode M of ion distribution is given by

$$G_M^{(TB)}(x) = -\frac{1}{2}\left(\frac{1}{\varepsilon_{in}} - \frac{1}{\varepsilon_w}\right)\sum_i \frac{q_i^2}{B_i} - \left(\frac{1}{\varepsilon_{in}} - \frac{1}{\varepsilon_w}\right)\sum_{i<j}\frac{q_i q_j}{f_{ij}} + \sum_{i<j}\frac{q_i q_j}{\varepsilon_{in} r_{ij}} \quad (1)$$

where

$$f_{ij} = \sqrt{r_{ij}^2 + B_i B_j \exp\left(-\frac{r_{ij}^2}{4B_i B_j}\right)} \quad (2)$$

and ε_{in} and ε_w are the dielectric constants (see the SI) of the nucleic acid and water, respectively, q_i and q_j are the phosphate or the ion charges, r_{ij} is the distance between q_i and q_j, and B_i and B_j are the Born radii of q_i and q_j, respectively (see Figure 1a). The Born radii can be evaluated from several different methods such as the HCT method.[43] In our calculation, we will first use the HCT method, which is computationally efficient. We will later perform calculations using other Born radii models to check the robustness of the results.

The Born radius reflects the solvent polarization (the first and second summations in eq 1) in excess of the dielectrically homogeneous system where water is replaced with DNA dielectrics (the last summation in eq 2). Here we assume that a hydrated ion, whose hydration layer contains structured water, has a similar dielectric constant ε_{in} as the DNA. As DNA helices move closer, water molecules between the helices are displaced and move to the outside region. This change of the distribution of water molecules leads to a weakened overall solvent polarization effect, as manifested by an increased Born radii for the charges (phosphates or ions, as shown in Figures 1bcd). Such a change is most significant for charges facing each other on the different DNA helices, e.g., the phosphate nos. 8, 9, 56, and 57 in Figure 1. Another notable phenomena is that the change in the Born radii for the TB ions are more pronounced for helices that are close to each other within a short distance (x < 30 Å), corresponding to a significant short-range solvent polarization effect.

General Properties of Free Energy Components. We here focus on the free energy profile (landscape), i.e., the x-dependence of the free energy, because the free energy landscape determines the mean force between the helices. In order to identify the different components in the interhelix interactions, we calculated the free energy profile for the system in three different types of solutions: (a) pure water, (b)

dx.doi.org/10.1021/jp4010955 | J. Phys. Chem. B 2013, 117, 7221−7227

monovalent ion solutions, and (c) Mg^{2+} and Mn^{2+} solutions. In section 2 of the SI, we show the results for pure water and monovalent ion solutions. Here we focus on the results for the Mg^{2+} and Mn^{2+} solutions. We focus on these two types of divalent ion solutions because they show contrastingly different interhelix forces in experiments.[14,16,17]

Our general strategy here is to investigate the free energy landscape for the different free energy components (see Figure 2): (a) The mean Coulomb energy $\Delta G_E(x)$ for the interaction

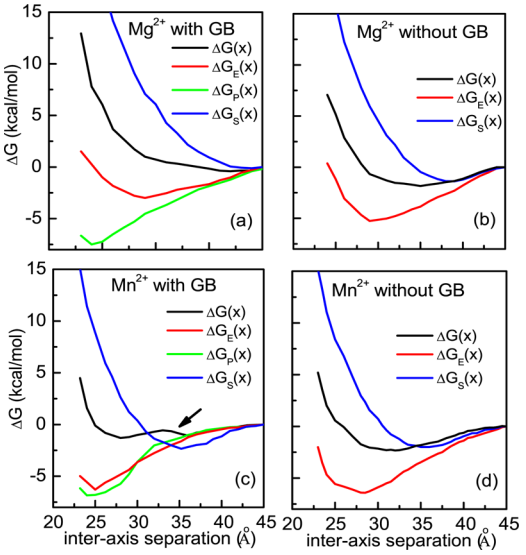

Figure 2. Free energy landscape and the component free energies in 10 mM $MgCl_2$ and 10 mM $MnCl_2$ solutions with (a and c) and without (b and d) solvent polarization (GB).

between the different charges; (b) The polarization energy $\Delta G_P(x)$ of the charges in the TB region; (c) The ion entropic free energy $\Delta G_S(x)$. The predicted x-dependence of the free energy for the different components (Figure 2a,c) shows several important features.

(1) As the helices move closer, the Coulomb energy $\Delta G_E(x)$ initially decreases due to the increased number of the TB ions and consequently the stronger ion correlation effect. For further smaller interhelix distance x's (<25 Å), $\Delta G_E(x)$ increases as x becomes smaller due to the Coulomb repulsion between the TB ions on the different helices.[9,10]

(2) As the helices move closer, the ion entropic free energy $\Delta G_S(x)$ for Mn^{2+} (Figure 2c) initially decreases and then increases for $x \leq 35$ Å. The nonmonotonic behavior is a result of the competition between two effects. As helices approach each other, more ions are attracted to the nucleic acid and become TB ions. This causes a larger net entropy decrease for the TB ions. However, more TB ions means stronger charge neutralization, which causes a more uniform ion distribution and hence a larger entropy for the diffusive ions. The competition between the above ion entropic effects results in a nonmonotonic behavior of the x-dependence of $\Delta G_S(x)$. The nonmonotonic behavior is less significant for bulkier Mg^{2+} ions (Figure 2a) due to the weaker ion-DNA interaction and the smaller number of bound ions (Figure 3) than the less bulky Mn^{2+} ions.

Solvent polarization can cause notable changes in the ion entropic free energy landscape $\Delta G_S(x)$. For Mg^{2+}, the solvent polarization effect causes the above nonmonotonic behavior of $\Delta G_S(x)$ to disappear (see Figure 2a). This is because the helices

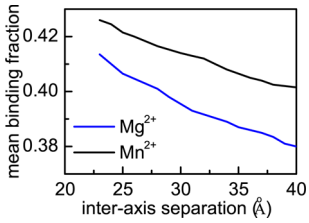

Figure 3. Mean number of bound ions per phosphate for 10 mM $MgCl_2$ and $MnCl_2$ (with solvent polarization effect).

are much less neutralized in a Mg^{2+} solution (especially with the solvent polarization/screening) than in a Mn^{2+} solution, thus, as helices move closer, the TB ion-induced increase of the diffusive ion entropy (decrease of $\Delta G_S(x)$) is less significant.

(3) The polarization free energy $\Delta G_P(x)$ decreases (see Figure 2a,c) as x decreases; see below for a more detailed discussion.

Solvent Polarization Effect. *Evidence for the Important Role of the Solvent Polarization Effect in Interhelix Interactions.* Without considering the solvent polarization effect (i.e., without invoking the GB model), For both $MgCl_2$ and $MnCl_2$ solutions, the free energy $\Delta G(x)$ (Figure 2b,d) gives an attractive interhelix force for $x \geq 30$ Å. As previously reported,[10] such an attraction can be attributed to the correlated organization of the TB ions on the different helices (see $\Delta G_E(x)$ curves in Figure 2b,d). The conclusion here, which is based on the atomistic structural model, agrees with the previous findings based on the coarse-grained structural model.[10] However, these solvent polarization-free predictions (for the attractive force) are not consistent with the experimental finding (no attractive force) for a Mg^{2+} solution. The result points to the possibly essential role of the solvent polarization effect.

In contrast to the above solvent polarization-free predictions, calculations with the solvent polarization effect lead to new predictions that are consistent with the experimental findings. For a Mg^{2+} solution, as shown by the $\Delta G(x)$ curve in Figure 2a, the attractive force predicted from the polarization-free calculation (Figure 2b) now disappears. In contrast, as shown in Figure 2c, for a Mn^{2+} solution, with the solvent polarization effect, $\Delta G(x)$ decreases as x decreases in the range 27 Å $\leq x \leq$ 33 Å, resulting in an attractive interhelix force. These predictions agree with the experimental findings.[14,16] The results here show that solvent polarization plays an important role in interhelix interaction. In the following, from the free energy landscape, we investigate how solvent polarization causes the different (repulsive vs attractive) forces in the different ionic solutions.

Free Energy Landscape for Solvent Polarization in the Different Ionic Solutions. The solvent polarization-assisted attractive/repulsive force is directly related to the steepness of the x-dependence of the polarization free energy $\Delta G_P(x)$. As x decreases, $\Delta G_P(x)$ in a Mn^{2+} solution shows a much steeper decrease than in a Mg^{2+} solution. For Mn^{2+}, the steep decrease of $\Delta G_P(x)$ in the range 27 Å $\leq x \leq$ 34 Å causes a decrease in the total free energy ΔG, resulting in an attractive interhelix force.[14,16] In what follows, we analyze the origin of the different behaviors of $\Delta G_P(x)$ for the two types of ions. The analysis may offer insights into the solvent polarization assisted interhelix attraction.

In order to identify the dominant polarization effect, in Figure 4a,b, we show the components of the polarization free

dx.doi.org/10.1021/jp4010955 | J. Phys. Chem. B 2013, 117, 7221−7227

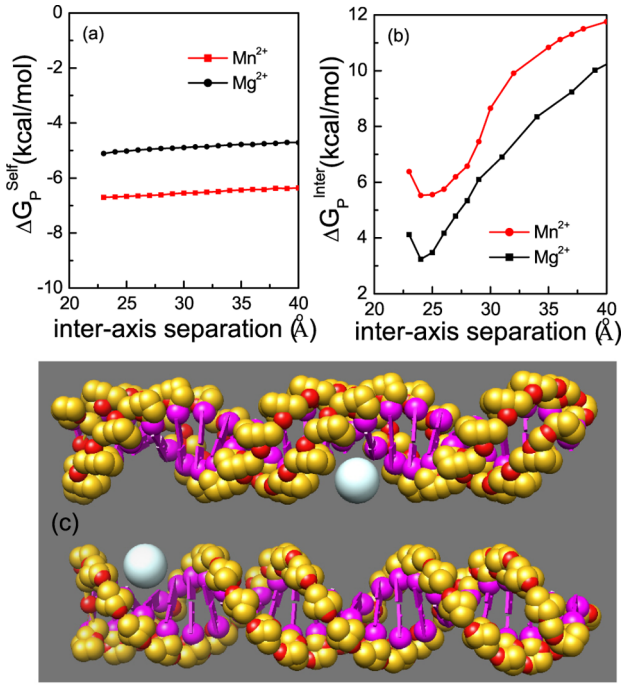

Figure 4. (a) Self-polarization energy of the bound ions for 10 mM $MgCl_2$ and $MnCl_2$ (the first summation in eq 1). (b) The charge−charge interaction energy for 10 mM $MgCl_2$ and $MnCl_2$ (the second and third summations in eq 1). (c) A 3D schematic diagram for the burial of ions in the (major) groove.

energy: self-polarization energy of the TB ions (the first summation in eq 1) and the polarization energy for the interactions between the TB ions and the phosphates (the rest two summations in eq 1) in 10 mM $MgCl_2$ and $MnCl_2$ solutions, respectively. As the two helices move closer, the self-polarization energy (Figure 4a) decreases slowly. The difference between the results for the Mg^{2+} and the Mn^{2+} solutions originates mainly from the different numbers of the bound ions (see Figure 3). For the interaction between the TB ions and the phosphates (Figure 4b), the polarization energy component drops with x much faster than the self-polarization energy. Moreover, in the range (27 Å ≤ x ≤ 34 Å) the energy drops much steeper for Mn^{2+} than for Mg^{2+}. These results suggest that the slope of the polarization free energy $\Delta G_P(x)$ profile (Figure 2a,c) is dominated by the interaction between the phosphates and the TB ions.

Origin of the Solvent Polarization-Assisted Interhelix Interaction. Physically, solvent polarization can reduce ion-phosphate attraction through dielectric screening. As helices move closer, the displacement of water from the region between the helices would weaken the overall dielectric screening (larger Born radii) and strengthen the ion-phosphate attraction. For Mn^{2+}, the steepest decent of $\Delta G_P(x)$ as the helices move closer occurs when the helix surface-to-surface distance is about 1−2 times the length of the diameters of the ion: 27 Å ≤ x ≤ 34 Å. In such a small-x regime, further decrease of x would greatly increase the probability for the TB ions to enter the grooves. The burial of the TB ions in the grooves would result in displacement of water molecules from the grooves and reduction in the solvent dielectric screening effect (i.e., increase in the Born radii). The above effect is more pronounced (see Figure 4c) for Mn^{2+} ions, which are less bulky than Mg^{2+} ions and hence can enter deeper into the grooves. In addition, Mn^{2+} has a much stronger interaction with the phosphate due to its smaller radius, therefore, Mn^{2+}−phosphate interaction is much more sensitive to the variation in the Born radii (polarization) than Mg^{2+}−phosphate interaction.

Integration of Ion Correlation and Solvent Polarization. Combing the different free energy components together, the interhelix attraction arises from two indispensable effects: (a) Coulombic correlation between the TB ions on the different helices and (b) solvent polarization effect. Both effects are important. Previous studies suggested that ignoring ion correlation leads to underestimation of the number of bound ions and underestimation of nucleic acids stability.[9,10,31,32] The current results further suggest that ion correlation can impact the polarization effect. Without ion correlation effect, the (underestimated) low number of the bound ions would result in a deficiency in the above bound ion-induced polarization effect and the reduction/disappearance of the attractive force. Reciprocally, without the polarization effect, ion correlation would be overestimated and as predicted by the previous polarization-free TBI model, the helices would show attraction for both Mg^{2+} and Mn^{2+} solutions, a result not consistent with the experimental finding.

Temperature Dependence of the Interhelix Force. To further compare our theoretical predictions with the experimental data, we calculated the osmotic pressure (see the SI for the details) for DNA double helices in the different $MgCl_2$ and $MnCl_2$ solutions and at different temperatures; see Figure 5a,b.

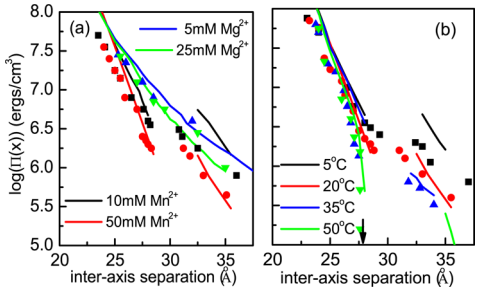

Figure 5. Predicted osmotic pressure from the (improved) TBI theory with the solvent polarization effect and the experimental data for the $MnCl_2$ and $MgCl_2$ solutions at 20 °C (a) and for the 10 mM $MnCl_2$ solution at the different temperatures (b). The symbols show the experimental data.[14,16] The same color of the symbols and curves denotes the same solution condition.

The theoretical predictions are generally consistent with the experimental results. The predicted osmotic pressure shows a repulsive force in the Mg^{2+} solution and a transition from the repulsive to the attractive forces in the Mn^{2+} solution. Specifically, in the 10 mM Mn^{2+} solution at 20 °C, we see an attractive force separated by a distance between 28 and 32.3 Å, which is roughly in the same range as the experimental range between 28.2 and 31.2 Å. The average theory-experiment difference in the attractive force range is around 20%. The theory-experiment difference may stem from several reasons such as the possible site-specific ion binding, the influence from the other nearby helices (many-body effect) and the use of the continuum solvent model. A higher ion concentration causes a lower entropic cost for ion binding, therefore, leads to more bound ions and a stronger ion correlation and solvent polarization effect. This would lead to a stronger attraction for the Mn^{2+} solution. Furthermore, As the temperature is increased, the solvent dielectric constant is smaller (see eq 1 in

dx.doi.org/10.1021/jp4010955 | J. Phys. Chem. B 2013, 117, 7221−7227

the SI). The decrease in the dielectric constant results in a stronger counterion-DNA interaction and thus more bound ions and stronger interhelix attraction for the Mn^{2+} solution. For example, at 50 °C (marked with green in Figure 5b), we find a strong and wide-range attraction.

3. DISCUSSION AND CONCLUSION

To summarize, ion correlation and solvent polarization effects can act together to cause an attractive force between DNA helices. Of particular interest here is the fact that ion-specific solvent polarization may play a critical role in modulating the electrostatic force between the helices. Specifically, compared to the (bulkier) Mg^{2+} ions, the (less bulky) Mn^{2+} ions can efficiently displace water from DNA helices and hence reduce the solvent polarization. This causes a net attractive interaction between the helices.

Compared to the previous studies,[6−12,18] the current model has the advantage of quantitatively accounting for Coulomb correlation, solvent polarization and all-atom nucleic acid structure in a consistent framework. However, as explained below, the current study, which is based on several important approximations, has limitations. The theory relies on the GB model to describe the solvent polarization effect. The GB model is a computationally efficient pairwise approximation for a continuum description of the solvent polarization effect. At the center of the GB model is the Born radii. There are a number of methods to evaluate the Born radii.[37,43−49] We here used the HCT method[43] to calculate the Born radii. To test the influence of the different Born radii model, we have also used two other methods (GBr^4 and GBr^6).[44,45] Our calculation shows that the Born radii from the HCT method are consistent with those obtained from the GBr^6 method[45] and are smaller than those from the GBr^4 method.[44] We note that the GBr^6 method enables an reduction in the error of the Coulomb-field approximation thus can reliably predict the Born radii.[45] As shown in Figure 5 in the SI, the HCT and the GBr^6 methods give consistent predictions for the free energy $\Delta G(x)$ for the helices in a 10 mM $MnCl_2$ solution at 20 °C, while the GBr^4 method gives much higher $\Delta G(x)$ and gives a strong repulsive interaction between the helices. The sensitivity on the Born radii further manifests the importance of water polarization in the interaction between the helices.

Besides the solvent polarization effect, there exist several other (nonexclusive) effects for the interhelix force. One of the notable effects is the disruption of the helix hydration layer.[14,16,17,20] This nonpolar contribution of the hydration as well as other effects such as the solvent dielectric saturation effect may also be important.[50] These effects are not explicitly accounted for in the current theory. As a crude estimation, we computed the nonpolar contribution of hydration by using the change of the solvent accessible surface area of the approaching helices upon ion binding. As shown in the SI (section 3), the nonpolar hydration free energy contribution is weaker than the Coulombic and polarization effects and the nonpolar effect becomes important only for $x \leq 25$ Å, which is out of (smaller than) the range of x wherein the interhelix attraction occurs.

In addition, we assume the ions to be hydrated. Dehydration of ions could occur when the interhelix distance becomes smaller than or comparable to the ion size.[2] The contributions from the above effects, especially from the nonpolar hydration effect, deserves a further detailed quantitative study. In addition, the information about the local changes in water polarization and structure around the bound counterions is much needed. Though the Born radii and the solvent accessible surface area indirectly reflect the change of water structure around the tightly bound ions and the helix, the current form of the model cannot directly probe the local changes in water polarization.

Nucleic acid interactions can be sensitive to the 3D structure, therefore, the conclusions derived here may not be applicable to RNA helices or other DNA helices such as triple-stranded helices (tsDNA). Experimental results suggested that, although DNA helices form insoluble condensation, RNA helices resist condensation.[17,19,51] Moreover, for triple-stranded DNA (tsDNA) helices in a Mg^{2+} ion solution,[27,28] interhelix attraction was observed, possibly due to the higher electric charge density of tsDNA which causes a stronger Mg^{2+}−DNA interaction and a stronger hydration force. Furthermore, the nucleic acid helices in a solution can be randomly oriented instead of perfectly aligned in parallel with each other. Previous studies suggest that the orientational sampling may reduce the magnitude of the interhelix force.[52,53]

The current form of the TBI model cannot treat more complex condensing agents such as trivalent cations, or polyamines or other larger ligands. Nucleic acids interactions with these ligands involve specific electrostatic and non-electrostatic interactions as well as the conformational flexibility of the ligands and requires a new theory. Another issue in the current model is the simplification of the charge distribution on the nucleic acids: charges on the oxygen atoms of the phosphate groups are collapsed to the phosphate atoms and the partial charges of neutral atoms are neglected. Even though the current TBI model may capture a significant portion of the physics in the problem, the above detailed charge distribution may also impact the interhelix interaction.

Despite the above limitations, the present quantitative study offers a useful estimation for the effects of solvent polarization and charge−charge electrostatic correlation in nucleic interactions.[16,25] Furthermore, the theory, which puts many-ion correlation and fluctuation, solvent polarization, and atomistic nucleic acid structures in a consistent framework, has the potential to be extended to treat more complex systems.

■ ASSOCIATED CONTENT

Supporting Information

Additional calculation results and parameters. This material is available free of charge via the Internet at http://pubs.acs.org.

■ AUTHOR INFORMATION

Corresponding Author

*E-mail: chenshi@missouri.edu.

Notes

The authors declare no competing financial interest.

■ ACKNOWLEDGMENTS

This research was supported by NSF Grants MCB0920067 and MCB0920411 and NIH Grant GM063732. Most of the numerical calculations involved in this research were performed on the HPC resources at the University of Missouri Bioinformatics Consortium (UMBC).

■ REFERENCES

(1) Gelbart, W.; Bruinsma, R.; Pincus, P.; Parsegian, V. DNA-Inspired Electrostatics. *Phys. Today* **2000**, *53*, 38−44. Solis, V.; Olvera de la Cruz, M. Flexible Polymers Also Counterattract. *Phys. Today* **2001**, *54*, 71−72.

(2) Bloomfield, V. A. DNA Condensation by Multivalent Cations. *Biopolymers* **1997**, *44*, 269−282. Draper, D. E. RNA Folding: Thermodynamic and Molecular Descriptions of the Roles of Ions. *Biophys. J.* **2008**, *95*, 5489−5495. Chen, S. RNA Folding: Conformational Statistics,Folding Kinetics, and Ion Electrostatics. *Annu. Rev. Biophys.* **2008**, *37*, 197−214.
(3) Russell, R.; Millett, I. S.; Tate, M. W.; et al. Rapid Compaction During RNA Folding. *Proc. Natl. Acad. Sci. U.S.A.* **2002**, *99*, 4266−4271.
(4) Hayes, R. L.; Noel, J. K.; Mohanty, U.; et al. Magnesium Fluctuations Modulate RNA Dynamics in the SAM-I Riboswitch. *J. Am. Chem. Soc.* **2012**, *134*, 12043−12053. Mak, C. H.; Henke, P. S. Ions and RNAs: Free Energies of Counterion-Mediated RNA Fold Stabilities. *J. Chem. Theory Comput.* **2013**, *9*, 621−639.
(5) Wong, G. C. L. Electrostatics of Rigid Polyelectrolytes. *Curr. Opin. Colloid Interface Sci.* **2006**, *11*, 310−315.
(6) Kjellander, R.; Marcelja, S. Correlation and Image Charge Effects in Electric Double Layer. *Chem. Phys. Lett.* **1984**, *112*, 49−53.
(7) Rouzina, I.; Bloomfield, V. A. Macroion Attraction Due to Electrostatic Correlation between Screening Counterions. 1. Mobile Surface-Adsorbed Ions and Diffuse Ion Cloud. *J. Phys. Chem.* **1996**, *100*, 9977−9989. Shklovskii, B. Wigner Crystal Model of Counterion Induced Bundle Formation of Rodlike Polyelectrolytes. *Phys. Rev. Lett.* **1999**, *82*, 3268−3271.
(8) Kirkwood, J. G.; Shumaker, J. B. The Influence of Dipole Moment Fluctuations on the Dielectric Increment of Proteins in Solution. *Proc. Natl. Acad. Sci. U.S.A.* **1952**, *38*, 855−862.
(9) Travesset, A.; Vaknin, D. Bjerrum Pairing Correlations at Charged Interfaces. *Europhys. Lett.* **2006**, *74*, 181−187.
(10) Tan, Z.; Chen, S. Ion-mediated Nucleic Acid Helix-Helix Interactions. *Biophys. J.* **2006**, *91*, 518−536.
(11) Olvera de la Cruz, M.; Belloni, L.; Delsanti, M.; et al. Precipitation of highly Charged Polyelectrolyte Solutions in the Presence of Multivalent Salts. *J. Chem. Phys.* **1995**, *103*, 5781−5790.
(12) Kornyshev, A.; Leikin, S. Electrostatic Zipper Motif for DNA Aggregation. *Phys. Rev. Lett.* **1999**, *82*, 4138−4144.
(13) Angelini, E. E.; Liang, H.; Wriggers, W.; Wong, G. C. L. Like-Charge Attraction between Polyelectrolytes Induced by Counterion Charge Density Waves. *Proc. Natl. Acad. Sci. U.S.A.* **2003**, *100*, 8634−8637.
(14) Rau, D. C.; Lee, B.; Parsegian, V. Measurement of the Repulsive Force between Polyelectrolyte Molecules in Ionic Solution: Hydration Forces between Parallel DNA Double Helices. *Proc. Natl. Acad. Sci. U.S.A.* **1984**, *81*, 2621−2625.
(15) Tan, Z.; Chen, S. Salt Contribution to RNA Tertiary Structure Folding Stability. *Biophys. J.* **2011**, *101*, 176−187.
(16) Rau, D. C.; Parsegian, V. Direct Measurement of the Intermolecular Forces between Counterion-Condensed DNA Double Helices. Evidence for Long Range Attractive Hydration Forces. *Biophys. J.* **1992**, *61*, 246−259. Rau, D. C.; Parsegian, V. Direct Measurement of Temperature-Dependent Solvation Forces between DNA Double Helices. *Biophys. J.* **1992**, *61*, 260−271.
(17) Li, L.; Pabit, S.; Meisburger, S.; Pollack, L. Double-Stranded RNA Resists Condensation. *Phys. Rev. Lett.* **2011**, *106*, 108101−108104.
(18) Boroudjerdi, H.; Kim, Y. W.; Naji, A.; et al. Statics and Dynamics of Strongly Charged Soft Matter. *Phys. Rep.* **2005**, *416*, 129−199.
(19) Wong, G. C. L.; Pollack, L. Electrostatics of Strongly Charged Biological Polymers: Ion-Mediated Interactions and Self-Organization in Nucleic Acids and Proteins. *Annu. Rev. Phys. Chem.* **2010**, *61*, 171−189.
(20) Mariani, P.; Saturni, L. Measurement of Intercolumnar Forces between Parallel Guanosine Four-Stranded Helices. *Biophys. J.* **1996**, *70*, 2867−2874.
(21) Qiu, X.; Andresen, K.; Kwok, L. W.; et al. Inter-DNA Attraction Mediated by Divalent Counterions. *Phys. Rev. Lett.* **2007**, *99*, 038104; Abrupt Transition from a Free, Repulsive to a Condensed, Attractive DNA Phase, Induced by Multivalent Polyamine Cations. *Phys. Rev. Lett.* **2008**, *101*, 228101−228104.
(22) Bai, Y.; Das, R.; Millett, I. S.; et al. Probing Counterion Modulated Repulsion and Attraction between Nucleic Acid Duplexes in Solution. *Proc. Natl. Acad. Sci. U.S.A.* **2005**, *102*, 1035−1040.
(23) Lee, K.; Borukhov, I.; Liu, A. J.; et al. Effect of Mono- and Multivalent Salts on Angle-Dependent Attractions Between Charged Rods. *Phys. Rev. Lett.* **2004**, *93*, 128101−128104.
(24) Moghaddam, S.; Caliskan, G.; Thirumalai, D.; et al. Metal Ion Dependence of Cooperative Collapse Transitions in RNA. *J. Mol. Biol.* **2009**, *393*, 753−764.
(25) Todd, B. A.; Parsegian, V.; Shirahata, A. Attractive Forces between Cation Condensed DNA Double Helices. *Biophys. J.* **2008**, *94*, 4775−4782. DeRouchey, J.; Parsegian, V.; Rau, D. C. Cation Charge Dependence of the Forces Driving DNA Assembly. *Biophys. J.* **2010**, *99*, 2608−2615.
(26) Qiu, X.; Rau, D. C.; Parsegian, V.; et al. Salt-Dependent DNA-DNA Spacings in Intact Bacteriophage Reflect Relative Importance of DNA Self-Repulsion and Bending Energies. *Phys. Rev. Lett.* **2011**, *106*, 028102−028105.
(27) Qiu, X..; Rau, D. C.; Parsegian, V. Divalent Counterion-Induced Condensation of Triple-Strand DNA. *Proc. Natl. Acad. Sci. U.S.A.* **2010**, *107*, 21482−21486.
(28) Chen, G.; Chen, S. Quantitative Analysis of the Ion-Dependent Folding Stability of DNA Triplexes. *Phys. Biol.* **2011**, *8*, 066006.
(29) Cherstvy, A. G. Electrostatic Interactions in Biological DNA-Related Systems. *Phys. Chem. Chem. Phys.* **2011**, *13*, 9942−9968.
(30) Kirmizialtin, S.; Pabit, S.; Meisburger, S.; Pollack, L.; Elber, R. RNA and Its Ionic Cloud: Solution Scattering Experiments and Atomically Detailed Simulations. *Biophys. J.* **2012**, *102*, 819−828.
(31) Grant, J. A.; Pickup, B. T.; Nicholls, A. A Smooth Permittivity Function for Poisson-Boltzmann Solvation Methods. *J. Comput. Chem.* **2001**, *22*, 608−640.
(32) Baker, N. A. Improving Implicit Solvent Simulations: a Poisson-Centric View. *Curr. Opin. Struct. Biol.* **2005**, *15*, 137−143.
(33) Tan, Z.; Chen, S. Electrostatic Correlations and Fluctuations for Ion Binding to a Finite Length Polyelectrolyte. *J. Chem. Phys.* **2005**, *122*, 044903.
(34) He, Z.; Chen, S. Predicting Ion-Nucleic Acid Interactions by Energy Landscape-Guided Sampling. *J. Chem. Theory Comput.* **2012**, *8*, 2095−2101.
(35) Lu, X.; Olson, W. 3DNA: a Software Pckage for the Analysis, Rebuilding and Visualization of Three-Dimensional Nucleic Acid Structures. *Nucleic Acids Res.* **2003**, *31*, 5108.
(36) Still, W.; Tempczyk, A.; Hawley, R.; Hendrickson, H. Semianalytical Treatment of Solvation for Molecular Mechanics and Dynamics. *J. Am. Chem. Soc.* **1990**, *112*, 6127−6129.
(37) Bashford, D.; Case, A. A. Generalized Born Models of Macromolecular Solvation Effects. *Annu. Rev. Phys. Chem.* **2000**, *51*, 129.
(38) Jayaram, B.; Liu, Y.; Beveridge, D. L. A Modification of the Generalized Born Theory for Improved Estimates of Solvation Energies and PK Shifts. *J. Chem. Phys.* **1998**, *109*, 1465.
(39) Simonson, T.; Brunger, A. T. Solvation Free Energies Estimated from Macroscopic Continuum Theory: An Accuracy Assessment. *J. Phys. Chem.* **1994**, *98*, 4683−4694.
(40) Levy, R.; Zhang, L.; Gallicchio, E.; et al. On the Nonpolar Hydration Free Energy of Proteins: Surface Area and Continuum Solvent Models for the Solute-Solvent Interaction Energy. *J. Am. Chem. Soc.* **2003**, *125*, 9523.
(41) Feig, M.; Brooks, C. Recent Advances in the Development and Application of Implicit Solvent Models in Biomolecule Simulations. *Curr. Opin. Struct. Biol.* **2004**, *14*, 217−224.
(42) Raschke, T. M.; Tsai, J.; Levitt, M. Free Energy Reconstruction From Nonequilibrium Single-Molecule Pulling Experiments. *Proc. Natl. Acad. Sci. U.S.A.* **2001**, *98*, 3965.
(43) Hawkins, G.; Cramer, C.; Truhlar, D. Pairwise Solute Descreening of Solute Charges from a Dielectric Medium. *Chem. Phys. Lett.* **1995**, *246*, 122−129. Liu, H.; Kuntz, I.; Zou, X. Pairwise

GB/SA Scoring Function for Structure-Based Drug Design. *J. Phys. Chem. B* **2004**, *108*, 5453−5462.
(44) Gallicchio, E.; Levy, R. M. AGBNP, An Analytic Implicit Solvent Model Suitable for Molecular Dynamics Simulations and High-Resolution Modeling. *J. Comput. Chem.* **2004**, *25*, 479−499.
(45) Tjong, H.; Zhou, H. GBr6: A Parameterization-Free, Accurate, Analytical Gneralized Born Method. *J. Phys. Chem. B* **2007**, *111*, 3055−3061.
(46) Scarsi, M.; Apostolakis, J.; Caflisch, A. Continuum Electrostatic Energies of Macromolecules in Aqueous Solutions. *J. Phys. Chem. A* **1997**, *101*, 8098−8106.
(47) Ghosh, A.; Rapp, C.; Friesner, R. Generalized Born Model Based on a Surface Integral Formulation. *J. Phys. Chem. B* **1998**, *102*, 10983−10990.
(48) Lee, M.; Salsbury, F.; Brooks, C. Novel Generalized Born Methods. *J. Chem. Phys.* **2002**, *11*, 10606.
(49) Zhang, W.; Hou, T.; Xu, X. New Born Radii Deriving Method for Generalized Born Model. *J. Chem. Inf. Model.* **2005**, *45*, 88−93.
(50) Gavryushov, S. Electrostatics of B-DNA in NaCl and $CaCl_2$ Solutions: Ion Size, Interionic Correlation, and Solvent Dielectric Saturation Effect. *J. Phys. Chem. B* **2008**, *112*, 8955−8965; Mediating Role of Multivalent Cations in DNA Electrostatics: An Epsilon-Modified PoissonBoltzmann Study of B-DNA B-DNA Interactions in Mixture of NaCl and $MgCl_2$ Solutions. *J. Phys. Chem. B* **2009**, *113*, 2160−2169.
(51) Kirmizialtin, S.; Silalahi, A.; Elber, R.; Fenley, M. The Ionic Atmosphere around A-RNA: Poisson-Boltzmann and Molecular Dynamics Simulations. *Biophys. J.* **2012**, *22*, 829−838.
(52) Bai, Y.; Chu, Y. b.; Lipfert, J.; Pande, V.; Hershlag, D.; Doniach, S. Critical Assessment of Nucleic Acid Electrostatics via Experimental and Computational Investigation of an Unfolded State Ensemble. *J. Am. Chem. Soc.* **2008**, *130*, 12334−12341.
(53) Tan, Z.; Chen, S. Ion-mediated RNA Structural Collapse: Effect of Spatial Confinement. *Biophys. J.* **2012**, *103*, 827−836.